https://doi.org/10.3311/PPci.38565

Periodica Polytechnica Civil Engineering, 69(2), pp. 580–592, 2025

Critical Buckling Investigation of Composite Beams Under Poisson's Effect Using Nonlocal and Higher-order Shear Deformation Theories

Mouloud Hamhami[1*], Noureddine Elmeiche[1], Ismail Mechab[1], Zouaoui R. Harrat[2], Fabrice Bernard[3]

[1] Laboratory of Civil Engineering and Environment, Djillali Liabes University, P.O.B. 89, 22000 Sidi Bel Abbes, Algeria
[2] Laboratoire des Structures et Matériaux Avancés dans le Génie Civil et Travaux Publics, Djillali Liabes University, P.O.B. 89, 22000 Sidi Bel Abbes, Algeria
[3] Laboratory of Civil Engineering and Mechanical Engineering, INSA Rennes, University of Rennes, 20, Avenue des Buttes de Coësmes 35700 Rennes, France
[*] Corresponding author, e-mail: mouloud.hamhami@univ-sba.dz

Received: 15 October 2024, Accepted: 02 February 2025, Published online: 19 February 2025

Abstract

This investigation addresses the study of the buckling of composite material beams with different stacking sequences using nonlocal theory. A rotational field was introduced along the width of the beam, considering Poisson's effect and higher-order transverse shear deformation theories with a new warping shape function. The equilibrium equations are derived analytically using the energy principle, and the numerical solution of these equations is based on energy minimization using the Ritz method. A comparative study with different higher-order deformation theories was conducted to calculate the dimensionless critical buckling of a symmetrically and asymmetrically cross-ply laminated composite beam for two types of materials. To examine the influence of the nonlocal effect on critical buckling, another study was carried out on an isotropic material beam using nonlocal theory for different slenderness ratios. The dimensionless critical buckling results show perfect agreement with and without nonlocal theory compared to previously available works in the literature. A detailed investigation of Poisson's effect on critical buckling demonstrated its significant influence in the case of short beams made of unidirectional composites and laminated composites with different fiber orientations.

Keywords

buckling analysis, composite material, beam theory, nonlocal theory, HSDT, Poisson's effect

1 Introduction

This study aims to contribute by simultaneously exploring the influence of two critical parameters on the buckling of composite beams, namely: the non-local effect and the Poisson's effect. While previous studies have examined these effects separately, no research to date has integrated these two parameters simultaneously in the analysis of composite beam buckling. Our aim is to provide a robust theoretical model for understanding and predicting the buckling behavior of composite beams under realistic conditions, where these effects are often present simultaneously.

Composite materials are heterogeneous assemblies of at least two immiscible components that exhibit a strong interpenetration capability. These components, such as polymers, metals, or ceramics, combine their properties to form a material that performs better than each component individually [1, 2]. The applications of composite materials are diverse, spanning sectors such as aerospace, automotive, and construction. However, these materials often present numerous imperfections or defects that significantly reduce their performance [3–5]. Delamination, which involves the separation of the layers of the composite and compromises structural integrity, as well as cracking due to extreme stresses and buckling under normal loads, are common issues [6, 7].

The critical buckling behavior of beams is a fundamental aspect of structural engineering, as it directly influences the stability and safety of structures. Many researches have put efforts toward understanding the buckling effect of composite beams. Galuppi and Roye-Carfagni [8] investigated the buckling behavior of simply supported three-layered

Cite this article as: Hamhami, M., Elmeiche, N., Mechab, I., Harrat, Z. R., Bernard, F. "Critical Buckling Investigation of Composite Beams Under Poisson's Effect Using Nonlocal and Higher-order Shear Deformation Theories", Periodica Polytechnica Civil Engineering, 69(2), pp. 580–592, 2025. https://doi.org/10.3311/PPci.38565

sandwich beams with a viscoelastic core subjected to compressive loads. They analyzed the phenomena of glassy, rubbery, and creep buckling across a range of load values. Eltaher et al. [9] investigated the static stability of unified composite beams subjected to varying axial loads, providing insight into the critical conditions for buckling. Sorrenti et al. [10] analyzed the static response and buckling loads of multilayered composite beams using the refined zigzag theory combined with the higher-order Haar wavelet method to improve accuracy in predicting structural behavior. Tiwari and Shaikh [11] examined the buckling and vibration characteristics of shape memory laminated composite beams under axially heterogeneous in-plane loads, particularly in the glass transition temperature region. Understanding the critical load at which buckling occurs is crucial for designing composite beams capable of withstanding various load conditions without structural failure.

One key factor affecting the buckling behavior of composite beams is Poisson's effect, which describes the phenomenon where materials expand or contract in directions perpendicular to the direction of loading. Barathan et al. [12] studied the nonlinear free flexural vibration behavior of variable stiffness composite laminated beams using a sinusoidal-based shear flexible structural theory, which incorporates Poisson's effect. Li et al. [13] further explored the free vibration response of layered composite beams through a refined higher-order model that includes transverse normal strain and Poisson's effect. The accuracy of their closed-form solution was verified against existing literature. Jun et al. [14] examined the linear frequency behavior of layered composite beams using Reddy's shear deformation theory, which accounts for parabolic transverse shear strain along the thickness direction. Their study analyzed the influence of material anisotropy, Poisson's effect, slenderness, and boundary conditions on the fundamental frequency of the structure. The consideration of these effects, particularly Poisson's effect, is crucial as they significantly impact the mechanical response of composite materials, especially under compressive loads, and must be addressed in buckling analysis.

To accurately predict the critical buckling behavior of composite material beams, advanced theoretical frameworks are necessary. Thai et al. [15] conducted a size-dependent isogeometric analysis of laminated composite plates using the nonlocal strain gradient theory, offering valuable insights into the influence of small-scale effects. Similarly, Thang et al. [16] applied nonlocal strain gradient theory to analyze functionally graded carbon nanotube-reinforced composite nanoshells, highlighting the significance of size effects in structures with double curvature. Moayedi et al. [17] explored the thermo-vibrational responses of laminated composite nanoshells using the nonlocal strain–stress gradient theory, combined with the generalized differential quadrature element method (GDQEM), to account for small-scale phenomena. Additionally, Li et al. [18] examined the vibration behavior of rotating composite nano-annular plates, employing nonlocal theory alongside various plate theories to capture the impact of size effects. Collectively, these studies underscore the crucial role of nonlocal theory in providing a more comprehensive understanding of material behavior, especially in materials where size effects are particularly pronounced. Additionally, higher-order shear deformation theories (HSDT) [19–25] offer improved accuracy over classical beam theories by accounting for transverse shear deformations and providing a more realistic representation of the beam's mechanical response.

Despite the advancements in the theoretical understanding of buckling phenomena, there remains a significant gap in research regarding the critical buckling of composite beams under the influence of Poisson's effect. The objective of this article is to investigate the influence of the Poisson effect on the critical buckling of short and long beams made of unidirectional and layered composite materials using nonlocal theory. A high-order shear deformation theory with a new shape function is developed without the use of a shear correction factor. Numerical solutions of the equilibrium equations are presented for a simply supported beam using the Rayleigh-Ritz method. The effects of fiber orientation, beam slenderness, and transverse shear are examined in detail to assess the significance of the proposed model.

2 Mathematical formulation

The higher-order shear models discussed in this study are defined based on a variational methodology and are subsequently variationally consistent.

Consider a rectangular beam with length 'L' and width 'b' and a constant thickness 'h' as represented in Fig. 1.

The chosen coordinate system (x, y and z) is positioned at the center of the beam, with the coordinate parameters defined such that:

$$0 \le x \le L, 0 \le y \le b \quad \text{and} \quad -h/2 \le z \le h/2$$

In the following development, elastic behavior of the materials is assumed, along with small displacements, rotations, and deformations, and a perfect bond between the layers. Based on plate theory, the assumed displacement field for

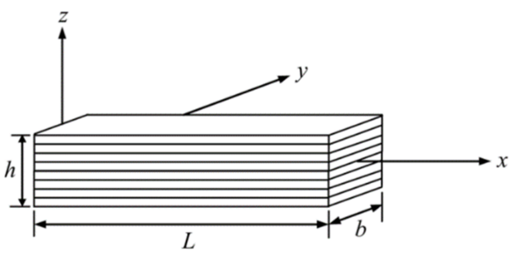

Fig. 1 Geometry of the beam

the composite beam, derived from a first-order shear deformation theory, can be expressed as shown in Eq. (1). These expressions have been previously stated by Jun et al. [14]:

$$U(x,z)=u(x)+z\varphi(x)+\big(f(z)-z\big)\left(\frac{\partial w(x)}{\partial x}+\varphi(x)\right)$$
$$V\pi(x,z)=f(z)\psi(x)$$
$$W(x,z)=w(x) \tag{1}$$

where U, V, and W are the displacements of an arbitrary point of the beam according to coordinates x, y, and z respectively. u and w are the displacements of a point on the mid-plane along the x and z directions respectively, and φ and ψ are the rotations of the normal to the mid-plane around the x and y axes respectively. The specified function $f(z)$ will determine the distribution of the shear stress across the thickness. The Euler-Bernoulli beam theory is a special case based on the kinematic function that cancels out, that is, $f(z) = 0$. The Timoshenko theory is simply obtained from the linear relationship:

$$f(z)=z \tag{2}$$

In this case, the shape factor κ_s is equal to one. As suggested, for example, in the literature, a factor κ_s close to 5/6 would be more relevant for Timoshenko beam theory. The higher-order shear beam model considered in this article develops a new shear function $f(z)$ proposed by Mechab et al. [26], which satisfies the following conditions:

$$f'(z)\big|_{z=\pm\frac{h}{2}}=0 \quad and \quad \int_{z=-\frac{h}{2}}^{z=\frac{h}{2}} f(z)\,dz=0\,, \tag{3}$$

where (') indicates differentiation with respect to z. The new shear strain function is presented below:

$$f(z)=h\sinh(z/h)e^{-\frac{\cosh(1/2)z^2}{\sinh(1/2)h^2}} \tag{4}$$

The strains associated with the displacements in Eq. (1) are:

$$\varepsilon_{xx}=\frac{\partial U}{\partial x}=\frac{\partial u}{\partial x}+z\frac{\partial\varphi}{\partial x}+\big(f(z)-z\big)\left(\frac{\partial^2 w}{\partial x^2}+\frac{\partial\varphi}{\partial x}\right)$$
$$\gamma_{xy}=\frac{\partial U}{\partial y}+\frac{\partial V}{\partial x}=f(z)\frac{\partial\psi}{\partial x}=z\frac{\partial\psi}{\partial x}+\big(f(z)-z\big)\frac{\partial\psi}{\partial x} \tag{5}$$
$$\gamma_{xz}=\frac{\partial U}{\partial z}+\frac{\partial W}{\partial x}=f'(z)\left(\frac{\partial w}{\partial x}+\varphi\right)$$

2.1 Nonlocal elasticity theory and constitutive relations

In local elasticity theory, the stress tensor at a material point is assumed to depend on the strain tensor at that point. However, in non-local elasticity theory, it is assumed that the stress tensor at a point depends on the strain tensor at all points in the continuum. According to Eringen's non-local elasticity theory [27], the non-local constitutive relations of a Hookean nanomaterial can be represented by the following constitutive differential relationship:

$$\left(1-\tau^2\ell^2\nabla^2\right)\sigma_{ij}^{NL}=\sigma_{ij}^{L}=C:\varepsilon,\left(\tau=\frac{e_0a}{\ell}\right) \tag{6}$$

For $\boldsymbol{i},\boldsymbol{j}=\boldsymbol{x},\boldsymbol{y},\boldsymbol{z}$.

The double dot represents the product, ε and C represent the components of strain and elastic constants, respectively. $\nabla^2=\partial^2/(\partial x^2)$ is the Laplacian operator. The non-local parameter e_0a has a dimension of length and can be greater than 1.

In the expression $\tau=(e_0a)/\ell\le 1$, the value of a depends on the internal length (granular distance, lattice parameter, distance between C-C bonds as molecular diameters, etc.), and ℓ is the external characteristic length (crack length or wavelength). e_0 is a constant specific to each material to adjust the model to obtain reliable results through experiments or other theories. σ_{ij}^{NL} and σ_{ij}^{L} represent the components of the non-local and local stress tensors, respectively, in the Cartesian coordinate system. By neglecting the components of transverse normal stress, the local constitutive relations can be expressed as follows:

$$\begin{Bmatrix}\sigma_{xx}^L\\ \sigma_{yy}^L\\ \tau_{xy}^L\\ \tau_{yz}^L\\ \tau_{xz}^L\end{Bmatrix}=\begin{bmatrix}\bar{C}_{11} & \bar{C}_{12} & \bar{C}_{16} & 0 & 0\\ \bar{C}_{12} & \bar{C}_{22} & \bar{C}_{26} & 0 & 0\\ \bar{C}_{16} & \bar{C}_{26} & \bar{C}_{66} & 0 & 0\\ 0 & 0 & 0 & \bar{C}_{44} & \bar{C}_{45}\\ 0 & 0 & 0 & \bar{C}_{45} & \bar{C}_{55}\end{bmatrix}\begin{Bmatrix}\varepsilon_{xx}^L\\ \varepsilon_{yy}^L\\ \gamma_{xy}^L\\ \gamma_{yz}^L\\ \gamma_{xz}^L\end{Bmatrix} \tag{7}$$

The material is orthotropic with respect to the original coordinate system; it follows that, under a rotation of an angle $\boldsymbol{\theta_k}$ around the z-axis in the x-y plane, the transformation formulas for the stiffnesses $\bar{\boldsymbol{C}}_{\boldsymbol{ij}}^{(\boldsymbol{k})}$ are of the form given by Zenkour [28]:

$$\begin{Bmatrix} \overline{C_{11}} \\ \overline{C_{12}} \\ \overline{C_{22}} \\ \overline{C_{16}} \\ \overline{C_{26}} \\ \overline{C_{66}} \end{Bmatrix} = \begin{bmatrix} c^4 & 2c^2s^2 & s^4 & 4c^2s^2 \\ c^2s^2 & c^4+s^4 & c^2s^2 & -4c^2-s^2 \\ s^4 & 2c^2s^2 & c^4 & 4c^2s^2 \\ -c^3s & cs\left(c^2-s^2\right) & cs^3 & 2cs\left(c^2-s^2\right) \\ -cs^3 & cs\left(s^2-c^2\right) & c^3s & 2cs\left(s^2-c^2\right) \\ c^2s^2 & -2c^2s^2 & c^2s^2 & \left(c^2-s^2\right)^2 \end{bmatrix} \begin{Bmatrix} C_{11} \\ C_{12} \\ C_{22} \\ C_{66} \end{Bmatrix}, \tag{8}$$

$$\begin{Bmatrix} \bar{C}_{44} \\ \bar{C}_{45} \\ \bar{C}_{55} \end{Bmatrix}^k = \begin{bmatrix} c^2 & s^2 \\ cs & -cs \\ s^2 & c^2 \end{bmatrix} \begin{Bmatrix} C_{44} \\ C_{55} \end{Bmatrix}$$

where $\boldsymbol{c = cos(\theta_k)}$ and $\boldsymbol{s = sin(\theta_k)}$. $\boldsymbol{C_{ij}}$ are the material stiffnesses (reduced to plane stresses) of the laminate:

$$\begin{gathered} C_{11} = \frac{E_x}{1-\nu_{xy}\nu_{yx}}, C_{12} = \frac{\nu_{yx}E_x}{1-\nu_{xy}\nu_{yx}} = \frac{\nu_{xy}E_y}{1-\nu_{xy}\nu_{yx}} \\ C_{22} = \frac{E_y}{1-\nu_{xy}\nu_{yx}}, C_{44} = G_{yz}, C_{55} = G_{xz}, C_{66} = G_{xy} \end{gathered} \tag{9}$$

In which $\boldsymbol{E_x}$ and $\boldsymbol{E_y}$ are the Young's moduli in the x and y directions of the material; $\boldsymbol{\nu_{xy}}$ and $\boldsymbol{\nu_{yx}}$ are the Poisson's ratios, and $\boldsymbol{G_{xy}}$, $\boldsymbol{G_{yz}}$, $\boldsymbol{G_{xz}}$ are the shear moduli in the x-y, y-z, and x-z planes, respectively.

The constitutive equations of laminated plates based on the higher-order shear deformation theory can be expressed as follows:

$$\begin{Bmatrix} N_{xx} \\ N_{yy} \\ N_{xy} \\ M_{xx} \\ M_{yy} \\ M_{xy} \\ S_{xx} \\ S_{yy} \\ S_{xy} \end{Bmatrix} = \begin{bmatrix} A_{11} & A_{12} & A_{16} & B_{11} & B_{12} & B_{16} & B_{11}^f & B_{12}^f & B_{16}^f \\ A_{12} & A_{22} & A_{26} & B_{12} & B_{22} & B_{26} & B_{12}^f & B_{22}^f & B_{26}^f \\ A_{16} & A_{26} & A_{66} & B_{16} & B_{26} & B_{66} & B_{16}^f & B_{26}^f & B_{66}^f \\ B_{11} & B_{12} & B_{16} & D_{11} & D_{12} & D_{16} & D_{11}^f & D_{12}^f & D_{16}^f \\ B_{12} & B_{22} & B_{26} & D_{12} & D_{22} & D_{26} & D_{12}^f & D_{22}^f & D_{26}^f \\ B_{16} & B_{26} & B_{66} & D_{16} & D_{26} & D_{66} & D_{16}^f & D_{26}^f & D_{66}^f \\ B_{11}^f & B_{12}^f & B_{16}^f & D_{11}^f & D_{12}^f & D_{16}^f & F_{11}^f & F_{12}^f & F_{16}^f \\ B_{12}^f & B_{22}^f & B_{26}^f & D_{12}^f & D_{22}^f & D_{26}^f & F_{12}^f & F_{22}^f & F_{26}^f \\ B_{16}^f & B_{26}^f & B_{66}^f & D_{16}^f & D_{26}^f & D_{66}^f & F_{16}^f & F_{26}^f & F_{66}^f \end{bmatrix} \begin{Bmatrix} \varepsilon_x^0 \\ \varepsilon_y^0 \\ \gamma_{xy}^0 \\ k_x^b \\ k_y^b \\ k_{xy}^b \\ k_x^s \\ k_y^s \\ k_{xy}^s \end{Bmatrix}, \tag{10}$$

$$\begin{Bmatrix} Q_{yz} \\ Q_{xz} \end{Bmatrix} = \begin{bmatrix} A_{44}^f & A_{45}^f \\ A_{45}^f & A_{55}^f \end{bmatrix} \begin{Bmatrix} \gamma_{yz}^s \\ \gamma_{xz}^s \end{Bmatrix}$$

where $\boldsymbol{N_{xx}}$, $\boldsymbol{N_{yy}}$ and $\boldsymbol{N_{xy}}$ are in-plane forces, $\boldsymbol{M_{xx}}$, $\boldsymbol{N_{yy}}$ and $\boldsymbol{M_{xy}}$ are the basic components of the stress resultants and moments, $\boldsymbol{S_{xx}}$, $\boldsymbol{S_{yy}}$ and $\boldsymbol{S_{xy}}$ are additional moment components associated with transverse shear effects, and $\boldsymbol{Q_{xy}}$, $\boldsymbol{Q_{yz}}$ are the transverse shear stress resultants. The stiffness coefficients of the laminate $\boldsymbol{A_{ij}}$ and $\boldsymbol{B_{ij}}$, etc., are defined in terms of the reduced stiffness coefficients $\boldsymbol{\bar{C}_{ij}^{(k)}}$ for the layers $k = 1, 2\ldots n$.

For ($i, j = 1, 2, 6$)

$$\begin{gathered} \left\{A_{ij}, B_{ij}, D_{ij}\right\} = \int_{-\frac{h}{2}}^{\frac{h}{2}} \left\{1, z, z^2\right\} \bar{C}_{ij} dz \\ \left\{B_{ij}^f, D_{ij}^f, F_{ij}^f\right\} = \int_{-\frac{h}{2}}^{\frac{h}{2}} \begin{Bmatrix} f(z) - z, z\left(f - (z) - z\right), \\ \left(f - (z) - z\right)^2 \end{Bmatrix} \bar{C}_{ij} dz \end{gathered} \tag{11}$$

For ($i, j = 4, 5$)

$$\left\{A_{ij}^f\right\} = \int_{-h/2}^{h/2} \kappa_s \left\{f'(z)^2\right\} \bar{C}_{ij} dz$$

And:

$$\begin{gathered} \varepsilon_x^0 = \frac{\partial u}{\partial x}, k_x^b = \frac{\partial \varphi}{\partial x},\ k_{xy}^b = \frac{\partial \psi}{\partial x},\ k_{xy}^s = \frac{\partial^2 w}{\partial x^2} + \frac{\partial \varphi}{\partial x} \\ k_x^s = \frac{\partial \psi}{\partial x},\ \gamma_{xz}^s = \frac{\partial w}{\partial x} + \varphi \end{gathered} \tag{12}$$

The mid-plane strains $\boldsymbol{\varepsilon_y^0}$ and $\boldsymbol{\gamma_{xy}^0}$, the bending curvature $\boldsymbol{k_y^b}$, and the higher order bending curvature $\boldsymbol{k_y^s}$ in Eq. (10) are not zero. Their expression is identified by assuming that $\boldsymbol{N_{yy}}$, $\boldsymbol{N_{xy}}$, $\boldsymbol{M_{yy}}$, $\boldsymbol{S_{yy}}$ and $\boldsymbol{Q_{yz}}$ are equal to zero.

Then, these strain components have been substituted into the expression of the non-zero forces ($\boldsymbol{N_{xx}}$, $\boldsymbol{M_{xx}}$, $\boldsymbol{M_{xy}}$, $\boldsymbol{S_{xx}}$ and $\boldsymbol{S_{xy}}$). Thus, Eq. (9) can be written as follows:

$$\begin{Bmatrix} N_{xx} \\ M_{xx} \\ M_{xy} \\ S_{xx} \\ S_{xy} \end{Bmatrix} = \begin{bmatrix} \overline{A_{11}} & \overline{B_{11}} & \overline{B_{16}} & \overline{B_{11}^f} & \overline{B_{16}^f} \\ \overline{B_{11}} & \overline{D_{11}} & \overline{D_{16}} & \overline{D_{11}^f} & \overline{D_{16}^f} \\ \overline{B_{16}} & \overline{D_{16}} & \overline{D_{66}} & \overline{D_{11}^f} & \overline{D_{66}^f} \\ \overline{B_{11}^f} & \overline{D_{11}^f} & \overline{D_{16}^f} & \overline{F_{11}^f} & \overline{F_{16}^f} \\ \overline{B_{16}} & \overline{D_{16}^f} & \overline{D_{66}^f} & \overline{F_{16}^f} & \overline{F_{66}^f} \end{bmatrix} \begin{Bmatrix} \varepsilon_x^0 \\ k_x^b \\ k_{xy}^b \\ k_x^s \\ k_{xy}^s \end{Bmatrix} \tag{13}$$

where:

$$\begin{bmatrix} \overline{A_{11}} & \overline{B_{11}} & \overline{B_{16}} & \overline{B_{11}^f} & \overline{B_{16}^f} \\ \overline{B_{11}} & \overline{D_{11}} & \overline{D_{16}} & \overline{D_{11}^f} & \overline{D_{16}^f} \\ \overline{B_{16}} & \overline{D_{16}} & \overline{D_{66}} & \overline{D_{11}^f} & \overline{D_{66}^f} \\ \overline{B_{11}^f} & \overline{D_{11}^f} & \overline{D_{16}^f} & \overline{F_{11}^f} & \overline{F_{16}^f} \\ \overline{B_{16}^f} & \overline{D_{16}^f} & \overline{D_{66}^f} & \overline{F_{16}^f} & \overline{F_{66}^f} \end{bmatrix} = \begin{bmatrix} A_{11} & B_{11} & B_{16} & B_{11}^f & B_{16}^f \\ B_{11} & D_{11} & D_{16} & D_{11}^f & D_{16}^f \\ B_{16} & D_{16} & D_{66} & D_{11}^f & D_{66}^f \\ B_{11}^f & D_{11}^f & D_{16}^f & F_{11}^f & F_{16}^f \\ B_{16}^f & D_{16}^f & D_{66}^f & F_{16}^f & F_{66}^f \end{bmatrix} - \begin{bmatrix} A_{12} & A_{16} & B_{12} & B_{12}^f \\ B_{12} & B_{16} & D_{12} & D_{12}^f \\ B_{26} & B_{66} & D_{26} & D_{26}^f \\ B_{12}^f & B_{16}^f & D_{12}^f & F_{12}^f \\ B_{26}^f & B_{66}^f & D_{26}^f & F_{26}^f \end{bmatrix}$$
$$\times \begin{bmatrix} A_{22} & A_{26} & B_{22} & B_{22}^f \\ A_{26} & A_{66} & B_{26} & B_{26}^f \\ B_{22} & B_{26} & D_{22} & D_{22}^f \\ B_{22}^f & B_{26}^f & D_{22}^f & F_{22}^f \end{bmatrix}^{-1} \times \begin{bmatrix} A_{12} & B_{12} & B_{26} & B_{12}^f & B_{26}^f \\ A_{16} & B_{16} & B_{66} & B_{16}^f & B_{66}^f \\ B_{12} & D_{12} & D_{26} & D_{12}^f & D_{26}^f \\ B_{12}^f & D_{12}^f & D_{26}^f & F_{12}^f & F_{26}^f \end{bmatrix} \tag{14}$$

In the case of laminated composite beams, the transverse shear force $\boldsymbol{Q_{yz} = 0}$ can be neglected. Using Eq. (10), the relationship between the transverse shear force and the deformation for the laminated composite beam can also be expressed as follows:

$$\begin{gathered} \gamma_{yz}^s = -\frac{A_{45}^f}{A_{44}^f}\gamma_{xz}^s \\ Q_{xz} = \left(A_{55}^f - \frac{A_{45}^{f\,2}}{A_{44}^f}\right)\gamma_{xz}^s = \bar{A}_{55}^f\gamma_{xz}^s \\ Q_{xz} = \bar{A}_{55}^f\left(\frac{\partial w}{\partial x} + \varphi\right) \end{gathered} \tag{15}$$

Using the non-local and local constitutive relations (6) and (7), the displacement relation (5), as well as the stress-strain relations based on linear elasticity theory, the resulting non-local stresses can be expressed in terms of the displacement and rotation components as follows:

$$\begin{Bmatrix} N_{xx} \\ M_{xx} \\ M_{xy} \\ S_{xx} \\ S_{xy} \end{Bmatrix} - (e_0 a)^2 \frac{\partial^2}{\partial x^2} \begin{Bmatrix} N_{xx} \\ M_{xx} \\ M_{xy} \\ S_{xx} \\ S_{xy} \end{Bmatrix} = \begin{bmatrix} \overline{A_{11}} & \overline{B_{11}} & \overline{B_{16}} & \overline{B_{11}^f} & \overline{B_{16}^f} \\ \overline{B_{11}} & \overline{D_{11}} & \overline{D_{16}} & \overline{D_{11}^f} & \overline{D_{16}^f} \\ \overline{B_{16}} & \overline{D_{16}} & \overline{D_{66}} & \overline{D_{11}^f} & \overline{D_{66}^f} \\ \overline{B_{11}^f} & \overline{D_{11}^f} & \overline{D_{16}^f} & \overline{F_{11}^f} & \overline{F_{16}^f} \\ \overline{B_{16}^f} & \overline{D_{16}^f} & \overline{D_{66}^f} & \overline{F_{16}^f} & \overline{F_{66}^f} \end{bmatrix} \begin{Bmatrix} \frac{\partial u}{\partial x} \\ \frac{\partial \varphi}{\partial x} \\ \frac{\partial \psi}{\partial x} \\ \frac{\partial^2 w}{\partial x^2} + \frac{\partial \varphi}{\partial x} \\ \frac{\partial \psi}{\partial x} \end{Bmatrix} \tag{16}$$

And:

$$Q_{xz} - (e_0 a)^2 \frac{\partial^2 Q_{xz}}{\partial x^2} = \bar{A}_{55}^f\left(\frac{\partial w}{\partial x} + \varphi\right) \tag{17}$$

2.2 Differential equations governing nonlocal elasticity

The differential equations governing equilibrium can be derived using the virtual displacement principle. The principle of virtual work in this case gives:

$$\pi = \frac{b}{2}\int_{-h/2}^{h/2}\int_S \begin{bmatrix} N_{xx}\varepsilon_x^0 + M_{xx}\kappa_x^b + M_{xy}\kappa_{xy}^b \\ +S_{xx}\kappa_x^s + S_{xy}\kappa_{xy}^s + Q_{xz}\gamma_{xz}^s \end{bmatrix} dx \tag{18}$$

$$T = \frac{1}{2}\int_0^L P\left[\frac{\partial w}{\partial x}\right]^2 dx \tag{19}$$

π is the elastic energy, T is the buckling energy, and P is the critical buckling load. The equilibrium equations for buckling are derived using the principle of conservation of energy as applied to a conservative system. The principle can be formulated as follows:

$$\int_{t_1}^{t_2}\delta\left(\pi - T\right)dt = 0 \tag{20}$$

By substituting Eqs. (5), (12), (18), and (19) into Eq. (20) and integrating across the thickness of the beam, Eq. (20) can be reformulated as follows:

$$\int_{-\frac{h}{2}}^{\frac{h}{2}}\int_\Omega \begin{bmatrix} N_{xx}\delta u_{,x} + M_{xx}\delta\varphi_{,x} + S_{xx}\left(\delta w_{,xx} + \delta\varphi_{,x}\right) \\ +M_{xy}\delta\psi_{,x} + S_{xy}\delta\psi_{,x} + Q_{xz}\delta\left(\delta w_{,x} + \delta\varphi\right) \end{bmatrix} dx - \int_0^L P w_{,x}\delta w_{,x} dx = 0 \tag{21}$$

Integrating Eq. (16) with respect toz gives:

$$\int_S \begin{bmatrix} N_{xx,x}\delta u + \left(M_{xx,x} + S_{xx,x} - Q_{xz}\right)\delta\varphi \\ +\left(S_{xx,xx} - Q_{xz,x} + P w_{,xx}\right)\delta w \\ +\left(M_{xy,x} + S_{xy,x}\right)\delta\psi \end{bmatrix} dx = 0 \tag{22}$$

The equilibrium equations can be derived from Eq. (22) by integrating the displacement gradients by parts and setting the coefficients δu, $\delta\varphi$, δw and $\delta\psi$ to zero separately:

$$\begin{aligned} &\delta u : \frac{\partial N_{xx}}{\partial x} = 0 \\ &\delta\varphi : \frac{\partial M_{xx}}{\partial x} + \frac{\partial S_{xx}}{\partial x} - Q_{xz} = 0 \\ &\delta w : \frac{\partial^2 S_{xx}}{\partial x^2} - \frac{\partial Q_{xz}}{\partial x} - P w_{,xx} = 0 \\ &\delta\psi : \frac{\partial M_{xy}}{\partial x} + \frac{\partial S_{xy}}{\partial x} = 0 \end{aligned} \tag{23}$$

With the boundary conditions:

$$\begin{aligned} &\left[N_{xx}\delta u_0\right]_0^L = 0, \left[\left(M_{xx} + S_{xx}\right)\delta\varphi\right]_0^L \\ &= 0, \left[S_{xx}\delta w_{,x}\right]_0^L = 0 \\ &\left[\left(Q_{xz} - S_{xx,x} + P\delta w_{,x}\right)\delta w\right]_0^L \\ &= 0, \left[\left(M_{xy} + S_{xy}\right)\delta\psi\right]_0^L = 0 \end{aligned} . \tag{24}$$

The in-plane force, the bending moment, and the additional stress couples associated with transverse shear effects are then given by:

$$\begin{aligned} &M_x = P\frac{\partial^4 w}{\partial x^4}\left(e_0 a\right)^4 + D_{11}\frac{\partial\varphi}{\partial x} + D_{11}^f\left(\frac{\partial^2 w}{\partial x^2} + \frac{\partial\varphi}{\partial x}\right) + \left(D_{16} + D_{16}^f\right)\frac{\partial\psi}{\partial x} \\ &+\left(A_{55}^f\left(\frac{\partial^2 w}{\partial x^2} + \frac{\partial\varphi}{\partial x}\right) - D_{11}^f\frac{\partial^3\varphi}{\partial x^3} - F_{11}^f\left(\frac{\partial^4 w}{\partial x^4} + \frac{\partial^3\varphi}{\partial x^3}\right) - \left(D_{16}^f + F_{16}^f\right)\frac{\partial^3\psi}{\partial x^3}\right)\left(e_0 a\right)^2 \\ &Q_{xz} - \frac{\partial S_{xx}}{\partial x} = \left(e_0 a\right)^2 P\frac{\partial^3 w}{\partial x^3} + A_{55}^f\left(\frac{\partial w}{\partial x} + \varphi\right) - D_{11}^f\frac{\partial^2\varphi}{\partial x^2} - F_{11}^f\left(\frac{\partial^3 w}{\partial x^3} + \frac{\partial^2\varphi}{\partial x^2}\right) - \left(D_{16}^f + F_{16}^f\right)\frac{\partial^2\psi}{\partial x^2} \\ &M_{xy} + P_{xy} = D_{16}\frac{\partial\varphi}{\partial x} + D_{16}^f\left(\frac{\partial^2 w}{\partial x^2} + \frac{\partial\varphi}{\partial x}\right) + \left(D_{66} + D_{66}^f\right)\frac{\partial\psi}{\partial x} + D_{16}^f\frac{\partial\varphi}{\partial x} + F_{16}^f\left(\frac{\partial^2 w}{\partial x^2} + \frac{\partial\varphi}{\partial x}\right) + \left(D_{66}^f + F_{66}^f\right)\frac{\partial\psi}{\partial x} \end{aligned} . \tag{25}$$

By substituting the above equations into the governing equations, we obtain the equilibrium equations associated with the present displacement field for the non-local beam:

$$
\begin{aligned}
&\overline{A_{11}}\frac{\partial^2}{\partial x^2}u+\overline{B_{11}}\frac{\partial^2}{\partial x^2}\varphi+\overline{B_{11}^f}\left(\frac{\partial^3}{\partial x^3}w+\frac{\partial^2}{\partial x^2}\varphi\right)+\left(\bar{B}_{16}+\bar{B}_{16}^f\right)\frac{\partial^2}{\partial x^2}\psi=0\\
&\left(e_0a\right)^4P\frac{\partial^5}{\partial x^5}w-\left(e_0a\right)^2\overline{B_{11}^f}\frac{\partial^4}{\partial x^4}u-\overline{D_{11}^f}\frac{\partial^4}{\partial x^4}\varphi-\overline{F_{11}^f}\frac{\partial^5}{\partial x^5}w-\overline{F_{11}^f}\frac{\partial^4}{\partial x^4}\varphi-\overline{F_{16}^f}\frac{\partial^4}{\partial x^4}\psi-\overline{D_{16}^f}\frac{\partial^4}{\partial x^4}\psi+\overline{A_{55}^f}\left(\frac{\partial^3}{\partial x^3}w+\frac{\partial^2}{\partial x^2}\varphi\right)\\
&+\overline{B_{11}}\frac{\partial^2}{\partial x^2}u+\overline{D_{11}^f}\frac{\partial^2}{\partial x^2}\phi+\overline{D_{11}^f}\frac{\partial^3}{\partial x^3}w+2\overline{D_{11}^f}\frac{\partial^2}{\partial x^2}\phi+2\overline{D_{16}^f}\frac{\partial^2}{\partial x^2}\psi-\left(e_0a\right)^2P\frac{\partial^3}{\partial x^3}w+\overline{B_{11}^f}\frac{\partial^2}{\partial x^2}u+\overline{F_{11}^f}\frac{\partial^3}{\partial x^3}w+\overline{F_{11}^f}\frac{\partial^2}{\partial x^2}\phi\\
&+\overline{F_{16}^f}\frac{\partial^2}{\partial x^2}\psi-\overline{A_{55}^f}\frac{\partial}{\partial x}\left(w+\phi\right)=0\\
&-\left(e_0a\right)^2P\frac{\partial^4}{\partial x^4}w+\overline{B_{11}^f}\frac{\partial^3}{\partial x^3}u+\overline{D_{11}^f}\frac{\partial^3}{\partial x^3}\varphi+\overline{F_{11}^f}\frac{\partial^4}{\partial x^4}w+\overline{F_{11}^f}\frac{\partial^3}{\partial x^3}\varphi+\overline{F_{16}^f}\frac{\partial^3}{\partial x^3}\psi+\overline{D_{16}^f}\frac{\partial^3}{\partial x^3}-\overline{A_{55}^f}\frac{\partial^2}{\partial x^2}w\\
&-\overline{A_{55}^f}\frac{\partial}{\partial x}\varphi+P\frac{\partial^2}{\partial x^2}w=0\\
&\overline{B_{16}^f}\frac{\partial^2}{\partial x^2}u+\overline{D_{16}}\frac{\partial^2}{\partial x^2}\varphi+\overline{D_{16}^f}\frac{\partial^3}{\partial x^3}w+2\overline{D_{16}^f}\frac{\partial^2}{\partial x^2}\phi+2\overline{D_{66}^f}\frac{\partial^2}{\partial x^2}\psi+\overline{D_{66}^f}\frac{\partial^2}{\partial x^2}\psi+\overline{B_{16}^f}\frac{\partial^2}{\partial x^2}u+\overline{F_{16}^f}\frac{\partial^3}{\partial x^3}w\\
&+\overline{F_{16}^f}\frac{\partial^2}{\partial x^2}\varphi+\overline{F_{66}^f}\frac{\partial^2}{\partial x^2}\psi=0
\end{aligned}
\tag{26}
$$

This tenth-order differential equation can also be expressed in matrix form as:

$$
\begin{bmatrix} L_{11} & L_{12} & L_{13} & L_{14}\\ L_{21} & L_{22} & L_{23} & L_{24}\\ L_{31} & L_{32} & L_{33} & L_{34}\\ L_{41} & L_{42} & L_{43} & L_{44}\end{bmatrix}\begin{Bmatrix}u\\ \varphi\\ w\\ \psi\end{Bmatrix}=\begin{Bmatrix}0\\0\\0\\0\end{Bmatrix}
\tag{27}
$$

[L] is the matrix of differential operators where:

$$
\begin{aligned}
&L_{11}=\bar{A}_{11}r^2\\
&L_{12}=\left(\bar{B}_{11}+\bar{B}_{11}^f\right)r^2\\
&L_{13}=\bar{B}_{11}^f r^3\\
&L_{14}=\left(\bar{B}_{16}+\bar{B}_{16}^f\right)r^2\\
&L_{21}=-\bar{B}_{11}^f\left(e_0a\right)^2r^4+\left(\bar{B}_{11}+\bar{B}_{11}^f\right)r^2\\
&L_{22}=-\left(\bar{D}_{11}^f+\bar{F}_{11}^f\right)\left(e_0a\right)^2r^4+\left(\left(e_0a\right)^2\bar{A}_{55}^f+2\bar{D}_{11}^f+\bar{F}_{11}^f+\bar{D}_{11}\right)r^2-\bar{A}_{55}^f\\
&L_{23}=\left(-\bar{F}_{11}^f\left(e_0a\right)^2+P\left(e_0a\right)^4\right)r^5+\left(+\bar{A}_{55}^f\left(e_0a\right)^2+P\left(e_0a\right)^2+\bar{D}_{11}^f+\bar{F}_{11}^f\right)r^3-\bar{A}_{55}^f r\\
&L_{24}=-\left(\bar{D}_{16}^f+\bar{F}_{16}^f\right)\left(e_0a\right)^2r^4+\left(\bar{D}_{16}+2\bar{D}_{16}^f+\bar{F}_{16}^f\right)r^2\\
&L_{31}=\left(\bar{B}_{11}^f\right)r^3\\
&L_{32}=\left(\bar{D}_{11}^f+\bar{F}_{11}^f\right)r^3-\bar{A}_{55}^f r\\
&L_{33}=\left(-P\left(e_0a\right)^2+\bar{F}_{11}^f\left(e_0a\right)^2\right)r^4+\left(-\bar{A}_{55}^f+P\right)r^2\\
&L_{34}=\left(\bar{D}_{16}^f+\bar{F}_{16}^f\right)r^3\\
&L_{41}=\left(\bar{B}_{16}+\bar{B}_{16}^f\right)r^2\\
&L_{42}=\left(\bar{D}_{16}+2\bar{D}_{16}^f+\bar{F}_{16}^f\right)r^2\\
&L_{43}=\left(\bar{D}_{16}^f+\bar{F}_{16}^f\right)r^3\\
&L_{44}=\left(\bar{D}_{66}+2\bar{D}_{66}^f+\bar{F}_{66}^f\right)r^2
\end{aligned}
\tag{28}
$$

where $r^n = \dfrac{d^n}{dx^n}$ is the differential operator.

2.3 Rayleigh-Ritz method

In this study, simply supported boundary conditions are examined. These boundary conditions are as follow:

At $x = 0$, L:

$$\begin{aligned} &U(0)=0,\ W(0)=0,\ S_{xx}(0)=0,\\ &M_{xx}(0)+S_{xx}(0)=0,\ M_{xy}(0)+S_{xy}(0)=0,\\ &U(L)=0,\ W(L)=0,\ S_{xx}(L)=0,\\ &M_{xx}(L)+S_{xx}(L)=0,\ M_{xy}(L)+S_{xy}(L)=0. \end{aligned} \tag{29}$$

The solution to the previous equations can be of the following form:

$$\begin{aligned} w(x) &= B_1 \cosh\left(\frac{\Phi_m x}{L}\right)+B_2\cos\left(\frac{\Phi_m x}{L}\right)\\ &-\mu_m\left(B_3\sinh\left(\frac{\Phi_m x}{L}\right)+B_4\sin\left(\frac{\Phi_m x}{L}\right)\right) \end{aligned} \tag{30}$$

Moreover, the axial mode shape function must satisfy the boundary conditions applied at the ends of the beam, which are $x = 0$ and $x = L$ (See Table 1).

3 Results and discussion

A study of the dimensionless critical buckling for a beam made of isotropic material without the Poisson effect and with the nonlocal effect is conducted. The beam is presented with different slenderness ratios (see Table 2). The present study was compared with different beam theories mentioned in Reddy's works [29]. The results show good agreement with the RBT model. The maximum error for a beam subjected to significant shear effects, with a ratio $L/h = 10$, does not exceed 1.59% for any nonlocal parameter. The error gradually decreases in proportion to the increase in slenderness and reaches a negligible value of 0.01%, with all results converging toward Euler's theory.

Table 1 Boundary conditions

Boundary conditions	B_i	Φ_m	μ_m
(S-S)	$B_1 = 0, B_2 = 0$ $B_3 = 0, B_4 = -1$	$m\pi$	1
(C-C)	$B_1 = 1, B_2 = -1$ $B_3 = 1, B_4 = -1$	$(2m + 1)\pi/2$	$\dfrac{\cos h\Phi_m - \cos\Phi_m}{\sin h\Phi_m - \sin\Phi_m}$
(C-S)	$B_1 = 1, B_2 = -1$ $B_3 = 1, B_4 = -1$	$(4m + 1)\pi/4$	$\dfrac{\cos h\Phi_m - \cos\Phi_m}{\sin h\Phi_m - \sin\Phi_m}$
(C-F)	$B_1 = 1, B_2 = -1$ $B_3 = 1, B_4 = -1$	$(2m - 1)\pi/2$	$\dfrac{\sin h\Phi_m - \sin\Phi_m}{\cos h\Phi_m + \cos\Phi_m}$

Another study on the dimensionless critical buckling of beams made of two symmetric composites of type (0/90/0) laminated in three layers and antisymmetric in two layers (0/90) is presented (see Tables 3 and 4). This study, utilizing a new warping shape function, was compared with different theories: The Parabolic Shear Deformation Theory (PSDT), the Hyperbolic Shear Deformation Theory (HSDT), the Exponential Shear Deformation theory (ESDT), and the First-Order Shear Deformation Theory (FSDT). The chosen shape functions are provided as follows:

- FSDT: $f(z) = z$
- PSDT: $f(z) = z\left(1-\dfrac{4z^2}{3h^2}\right)$
- HSDT: $f(z) = h\sinh(z/h) - z\cosh(1/2)$
- ESDT: $f(z) = z\exp\left[-2(z/h)^2\right]$

The results of this study for the two materials presented in Tables 3 and 4 show good agreement with the various deformation theories, with an error not exceeding 0.06% for the short beam ($L/h = 5$) and 0.04% for the slender beam ($L/h = 20$).

The properties of the chosen materials are as follows:

- Material I: E_1/E_2 = Open, $G_{12} = G_{13} = 0.6 \times E_2$, $G_{23} = 0.5 \times E_2$, $v_{12} = 0.25$.
- Material II: E_1/E_2 = Open, $G_{12} = G_{13} = 0.5 \times E_2$, $G_{23} = 0.2 \times E_2$, $v_{12} = 0.25$.

A detailed study using the new shear function to demonstrate the influence of the Poisson effect on the critical buckling load of a unidirectional orthotropic composite beam with the material listed below as material 3: G_{11} = 144.80 GPa; E_{22} = 9.65 GPa; G_{23} =3.45 GPa; $G_{12} = G_{13}$ = 4.14 GPa; $v_{12} = 0.3$ et L = 381 mm.

For different ply orientations from 0° to 90° (see Fig. 2), the critical buckling load decreases non-linearly, both with and without Poisson's effect, depending on the ply orientation, with maximum and minimum values observed at 0° and 90°, respectively. This observation holds true for the different slenderness ratios studied. The curves clearly illustrate the Poisson effect, especially at $\theta = 20°$. The amplitude of variation is maximal at 50.34% for the short beam ($L/h = 5$) and lower at 1.62% for the slender beam ($L/h = 20$). The superposition of the curves at 0° and 90° ply orientations is due to the null values of the stiffness terms $\overline{C_{16}} = \overline{C_{26}} = \overline{C_{45}}$. The discrepancy in critical buckling

Table 2 Dimensionless buckling loads for a pinned-pinned beam (L = 10, $E = 30 \times 10^6$, v = 0.3, $\bar{N}_{cr}^{0} = P \times (L^2 / EI)$)

	Nonlocal	Theories					
L/h	$\mu = (e_0 a)^2$	EBT	TBT	LBT	RBT	Present	Error (%)
	0	9.8696	9.6227	9.6630	9.6228	9.6242	1.47%
	0.5	9.4055	9.1701	9.2085	9.1702	9.1716	1.54%
	1	8.9830	8.7583	8.7949	8.7583	8.7597	1.56%
	1.5	8.5969	8.3818	8.4169	8.3819	8.3831	1.48%
	2	8.2426	8.0364	8.0700	8.0364	8.0376	1.55%
10	2.5	7.9163	7.7183	7.7506	7.7183	7.7195	1.56%
	3	7.6149	7.4244	7.4555	7.4245	7.4256	1.46%
	3.5	7.3356	7.1521	7.1820	7.1521	7.1532	1.58%
	4	7.0761	6.8990	6.9279	6.8991	6.9001	1.51%
	4.5	6.8343	6.6633	6.6912	6.6633	6.6644	1.59%
	5	6.6085	6.4431	6.4701	6.4432	6.4442	1.48%
	0	9.8696	9.8067	9.8171	9.8067	9.8071	0.38%
	0.5	9.4055	9.3455	9.3554	9.3455	9.3459	0.40%
	1	8.9830	8.9258	8.9352	8.9258	8.9261	0.34%
	1.5	8.5969	8.5421	8.5512	8.5421	8.5424	0.37%
	2	8.2426	8.1900	8.1988	8.1900	8.1904	0.44%
20	2.5	7.9163	7.8659	7.8742	7.8659	7.8662	0.35%
	3	7.6149	7.5664	7.5744	7.5664	7.5667	0.36%
	3.5	7.3356	7.2889	7.2966	7.2889	7.2891	0.33%
	4	7.0761	7.0310	7.0385	7.0310	7.0312	0.35%
	4.5	6.8343	6.7907	6.7979	6.7907	6.7910	0.41%
	5	6.6085	6.5663	6.5733	6.5663	6.5666	0.44%
	0	9.8696	9.8671	9.8675	9.8671	9.8671	0.01%
	0.5	9.4055	9.4031	9.4035	9.4031	9.4031	0.04%
	0.1	8.9830	8.9807	8.9811	8.9807	8.9807	0.03%
	1.5	8.5969	8.5947	8.5950	8.5947	8.5947	0.01%
	2	8.2426	8.2405	8.2408	8.2405	8.2405	0.02%
100	2.5	7.9163	7.9143	7.9146	7.9143	7.9143	0.01%
	3	7.6149	7.6130	7.6133	7.6130	7.6130	0.03%
	3.5	7.3356	7.3337	7.3340	7.3337	7.3337	0.06%
	4	7.0761	7.0743	7.0746	7.0743	7.0743	0.03%
	4.5	6.8343	6.8325	6.8328	6.8325	6.8325	0.05%
	5	6.6085	6.6068	6.6070	6.6068	6.6068	0.04%

Error (%) = 100*(Present- RBT)/ RBT, $\mu = (e_0 a)$ 2 is nonlocal parameter, (EBT: Euler-Bernoulli beam theory, TBT: Timoshenko beam theory, RBT: Reddy beam theory, LBT: Levinson beam theory) see [29]

loads with and without the Poisson effect is caused by the introduction in this study of the combined deformation of transverse shear in the yz-plane and transverse shear deformation in the xz-plane. Additionally, the axial deformation along the y-axis, as well as the bending moment curvature and additional moments with respect to the yy-axis, contribute to the development of this discrepancy.

Fig. 3 shows the variation of the dimensionless critical buckling load of the unidirectional orthotropic composite material made from Material I, as a function of slenderness ratio for different nonlocal parameters, considering the Poisson effect. The critical buckling load increases proportionally with the geometric ratio L/h and tends toward the limiting value of Euler's critical buckling. For a significant shear effect (L/h = 2.5), the critical buckling load with a nonlocal parameter varying from 1 to 5 decreases progressively by 61% to 89% compared to the critical buckling load without the nonlocal effect (μ = 0).

Table 3 Critical buckling loads λ for three-layer (0/90/0) symmetric cross-ply beams with different theories

Type	Theories	$L/h = 5$		$L/h = 20$	
		Material I	Material II	Material I	Material II
$E_1/E_2 = 10$	Present	4.734	3.653	7.666	7.437
	PSDBT	4.726	3.728	7.666	7.459
	HSDBT	4.727	3.731	7.666	7.461
	ESDBT	4.733	3.652	7.666	7.437
	FSDBT	9.797	7.605	27.854	26.500
	Error(%)	0.02%	0.03%	0.00%	0.00%
$E_1/E_2 = 40$	Present	8.699	5.803	27.092	24.450
	PSDBT	8.613	5.896	27.084	24.685
	HSDBT	8.611	5.902	27.087	24.696
	ESDBT	8.699	5.803	27.084	24.449
	FSDBT	9.797	7.605	27.854	26.500
	Error(%)	0.00%	0.00%	0.03%	0.00%

Error (%) = 100* (Present-ESDBT)/ESDBT

Table 4 Critical buckling loads λ for two-layer (0/90) antisymmetric cross-ply beams with different theories

Type	Theories	$L/h = 5$		$L/h = 20$	
		Material I	Material II	Material I	Material II
$E_1/E_2 = 10$	Present	1.929	1.779	2.242	2.228
	PSDBT	1.919	1.765	2.241	2.226
	HSDBT	1.919	1.765	2.241	2.226
	ESDBT	1.928	1.778	2.241	2.228
	FSDBT	1.945	1.800	2.243	2.228
	Error(%)	0.05%	0.06%	0.04%	0.00%
$E_1/E_2 = 40$	Present	3.976	3.461	5.304	5.237
	PSDBT	3.906	3.376	5.296	5.225
	HSDBT	3.903	3.372	5.296	5.224
	ESDBT	3.976	3.461	5.304	5.236
	FSDBT	3.891	3.349	5.296	5.224
	Error(%)	0.00%	0.00%	0.00%	0.02%

Error (%) = 100* (Present-ESDBT)/ESDBT

This variation is significant due to the warping effect of the beam's cross-section in both the *xz* and *yz* planes.

In the case of the two-layer antisymmetric composite shown in Fig. 4, the dimensionless critical buckling load decreases non-linearly for all beams with the slenderness ratios studied, with a maximum variation at the 0° ply orientation and tending toward a limit at the 90° ply. The nonlocal effect tends to become insignificant for slender beams, with the curves overlapping for the different values of the nonlocal effect.

Fig. 5 represents the dimensionless variation of the critical buckling load as a function of the central ply orientation

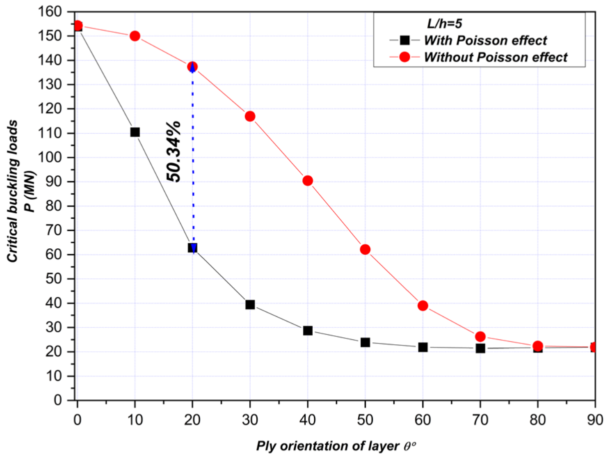

(a)

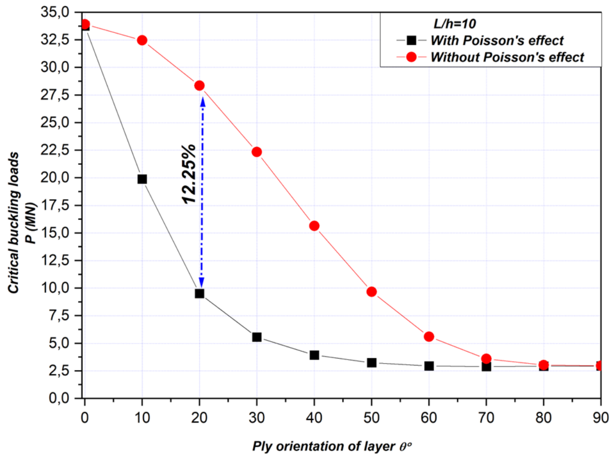

(b)

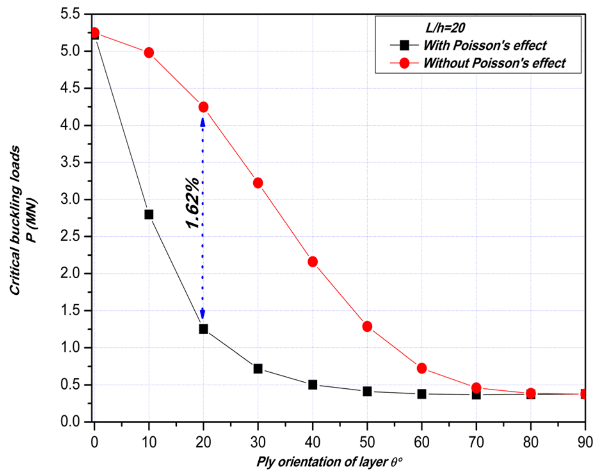

(c)

Fig. 2 Poisson's effect influence on the critical buckling load of a unidirectional orthotropic composite beam for different slenderness ratios, (a) $L/h = 5$, (b) $L/h = 10$, (c) $L/h = 20$

of a four-ply composite, considering the Poisson effect, for different slenderness ratios and nonlocal effect parameters. It is observed that the buckling load decreases linearly for short beams (L/h = 5 and 10), with constant

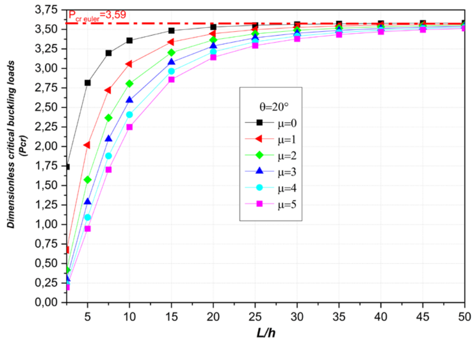

Fig. 3 Critical buckling variation load for different slenderness ratios considering different nonlocal coefficient and Poisson's effect

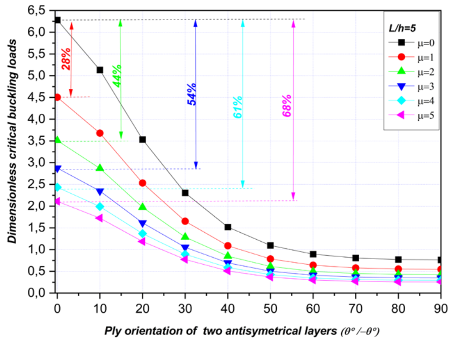

(a)

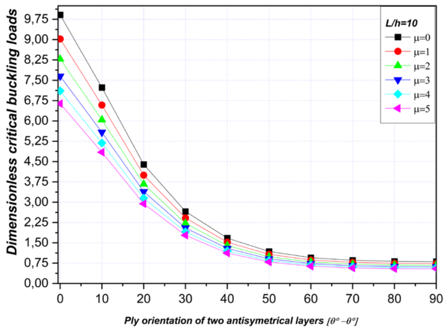

(b)

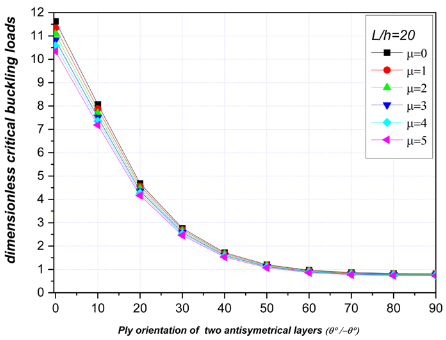

(c)

Fig. 4 Critical buckling variation load as a function of ply orientation for an antisymmetric composite beam (θ, -θ) for different nonlocal coefficient and slenderness ratios considering Poisson's effect, (a) L/h = 5, (b) L/h = 10, (c) L/h = 20

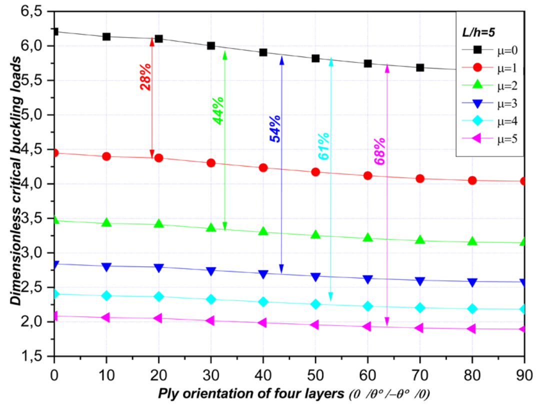

(a)

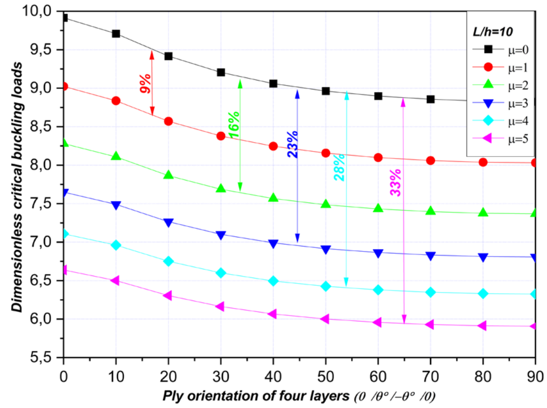

(b)

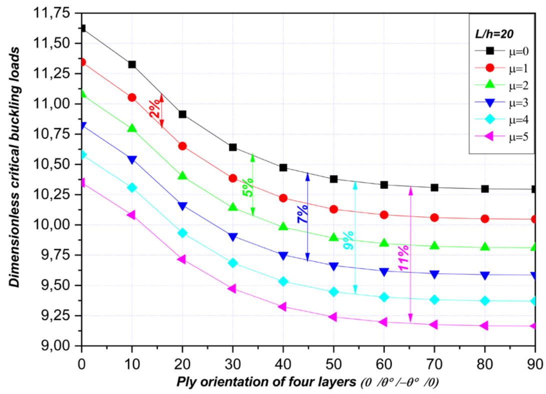

(c)

Fig. 5 Critical buckling variation load as a function of the central ply orientation in a four-ply composite beam for different nonlocal coefficient and slenderness ratios considering Poisson's effect, (a) L/h = 5, (b) L/h = 10, (c) L/h = 20

differences between the nonlocal curves and the reference curve (μ = 0), ranging from 28% to 68% and 9% to 33%, respectively. The decrease is almost linear for the slender beam (L/h = 20), varying from 2% to 11%. The nonlocal effect is significant for short beams and less pronounced for slender beams across all central ply orientations.

4 Conclusions

This study focuses on the analysis of the buckling of composite material beams using Eringen's nonlocal theory. A higher-order displacement field model is employed, which integrates transverse shear along the width of the beam, while accounting for the Poisson effect. A new warping shape function is introduced to enhance the accuracy of the analysis. The equilibrium equations, derived analytically using the energy principle, are solved numerically through the Ritz method based on the principle of energy minimization and the model is validated against previous studies. Here are the key findings:

- The results show good agreement with Reddy's model, with minimal differences for short beams, which become negligible for longer beams.
- The Poisson effect is maximized for short beams due to the influence of transverse deformation, which decreases with increasing slenderness. It is noted that for ply orientations of 20°, the Poisson effect is most significant.
- The critical buckling with a nonlocal effect (μ varying from 1 to 5) gradually decreases by 61% to 89% compared to critical buckling without the nonlocal effect ($\mu = 0$). Moreover, the nonlocal effect becomes more significant for short beams due to shear effects.
- The nonlocal effect tends to become insignificant for slender beams, with the curves for different nonlocal values converging.
- It is observed that the variation of the dimensionless critical load for a two-layer antisymmetric laminate is nonlinear regardless of slenderness, whereas this variation for a four-layer antisymmetric laminate is almost linear.

These results not only validate the applicability of nonlocal elasticity theory in composite structures but also highlight the importance of considering both material properties and geometry in the design of lightweight and high-performance structural elements.

References

[1] Aydogdu, M. "Buckling analysis of cross-ply laminated beams with general boundary conditions by Ritz method", Composites Science and Technology, 66(10), pp. 1248–1255, 2006. https://doi.org/10.1016/j.compscitech.2005.10.029

[2] Li, D., Nie, J-H., Wang, H., Yan, J-B., Hu, C-X., Shen, P. "Damage location, quantification and characterization of steel-concrete composite beams using acoustic emission", Engineering Structures, 283, 115866, 2023. https://doi.org/10.1016/j.engstruct.2023.115866

[3] Zhang, B., Chen, W., Xu, J. "Mechanical Behavior of Prefabricated Composite Box Girders with Corrugated Steel Webs under Static Loads", Journal of Bridge Engineering, 23(10), 04018077, 2018. https://doi.org/10.1061/(ASCE)BE.1943-5592.0001290

[4] Lam, H., Lin, W. Yoda, T. "Performance of Composite Twin I-Girder Bridges with Fatigue-Induced Cracks", Journal of Bridge Engineering, 22(9), 04017056, 2017. https://doi.org/10.1061/(ASCE)BE.1943-5592.0001094

[5] Su, Q-T., Yang, G-T., Wu, C. "Experimental investigation on inelastic behavior of composite box girder under negative moment", International Journal of Steel Structures, 12(1), pp. 71–84, 2012. https://doi.org/10.1007/s13296-012-1007-0

[6] Liu, T., Hai, M., Zhao, M. H. "Delaminating buckling model based on nonlocal Timoshenko beam theory for micro wedge indentation of a film/substrate system", Engineering Fracture Mechanics, 75(17), pp. 4909–4919, 2008. https://doi.org/10.1016/j.engfracmech.2008.06.021

[7] Evans, A. G., Hutchinson, J. W. "On the mechanics of delamination and spalling in compressed films", International Journal of Solids and Structures, 20(5), pp. 455–466, 1984. https://doi.org/10.1016/0020-7683(84)90012-X

[8] Galuppi, L., Royer-Carfagni, G. "Buckling of Three-layered Composite Beams with Viscoelastic Interaction", Composite Structures, 107, pp. 512–521, 2014. https://doi.org/10.1016/j.compstruct.2013.08.006

[9] Eltaher, M. A., Mohamed, S. A., Melaibari, A. "Static Stability of a Unified Composite Beams Under Varying Axial Loads", Science China Technological Sciences, 147, 106488, 2020. https://doi.org/10.1016/j.tws.2019.106488

[10] Sorrenti, M., Di Sciuva, M., Majak, J., Auriemma, F. "Static Response and Buckling Loads of Multilayered Composite Beams Using the Refined Zigzag Theory and Higher-Order Haar Wavelet Method", Mechanics of Composite Materials, 57, pp. 1–18, 2021. https://doi.org/10.1007/s11029-021-09929-2

[11] Tiwari, N., Shaikh, A. A. "Buckling and vibration analysis of shape memory laminated composite beams under axially heterogeneous in-plane loads in the glass transition temperature region", Discover Applied Sciences, 3(4), 451, 2021. https://doi.org/10.1007/s42452-021-04438-2

[12] Barathan, V., Rajamohan, V., Haboussi, M., Manickam, G. "Variable stiffness composite laminated beams—Nonlinear free flexural vibration behavior using a sinusoidal based shear flexible structural theory accounting for Poisson's effect", International Journal of Non-Linear Mechanics, 146, 104146, 2022. https://doi.org/10.1016/j.ijnonlinmec.2022.104146

[13] Li, J., Huo, Q., Li, X., Kong, X., Wu, W. "Vibration analyses of laminated composite beams using refined higher-order shear deformation theory", International Journal of Mechanics and Materials in Design, 10(1), pp. 43–52, 2014. https://doi.org/10.1007/s10999-013-9229-7

[14] Jun, L., Xiaobin, L., Hongxing, H. "Free vibration analysis of third-order shear deformable composite beams using dynamic stiffness method", Archive of Applied Mechanics, 79(12), pp. 1083–1098, 2009.
https://doi.org/10.1007/s00419-008-0276-8

[15] Thai, C. H., Nguyen-Xuan, H., Phung-Van, P. "A size-dependent isogeometric analysis of laminated composite plates based on the nonlocal strain gradient theor", Engineering with Computers, 39(1), pp. 331–345, 2022.
https://doi.org/10.1007/s00366-021-01559-5

[16] Thang, P. T., Tran, P., Nguyen-Thoi, T. "Applying nonlocal strain gradient theory to size-dependent analysis of functionally graded carbon nanotube-reinforced composite nanoplates", Applied Mathematical Modelling, 93, pp. 775–791, 2021.
https://doi.org/10.1016/j.apm.2021.01.001

[17] Moayedi, H., Ebrahimi, F., Habibi, M., Safarpour, H., Foong, L. K. "Application of nonlocal strain–stress gradient theory and GDQEM for thermo-vibration responses of a laminated composite nanoshell", Engineering with Computers, 37(4), pp. 3359–3374, 2021.
https://doi.org/10.1007/s00366-020-01002-1

[18] Li, H., Wang, W., Yao, L. "Analysis of the Vibration Behaviors of Rotating Composite Nano-Annular Plates Based on Nonlocal Theory and Different Plate Theories", Applied Sciences, 12(1), 230, 2022.
https://doi.org/10.3390/app12010230

[19] Prado Leite, L. F., da Rocha, F. C. "A Novel Higher-Order Zigzag Function Applied to Refined Unified Beam Theory for the Analysis of Composite Laminated Materials", Periodica Polytechnica Civil Engineering, 67(3), pp. 867–874, 2023.
https://doi.org/10.3311/PPci.21784

[20] Souad, H., Ismail, M., Hichem, A., Noureddine, E. "Vibration Analysis of Viscoelastic FGM Nanoscale Plate Resting on Viscoelastic Medium Using Higher-order Theory", Periodica Polytechnica Civil Engineering, 65(1), pp. 255–275, 2021.
https://doi.org/10.3311/PPci.16010

[21] Benfrid, A., Benbakhti, A., Harrat, Z. R., Chatbi, M., Krour, B., Bouiadjra, M. B. "Thermomechanical Analysis of Glass Powder Based Eco-concrete Panels: Limitations and Performance Evaluation", Periodica Polytechnica Civil Engineering, 67(4), pp. 1284–1297, 2023.
https://doi.org/10.3311/PPci.22781

[22] Thai, H. T., Choi, D. H. "Improved refined plate theory accounting for effect of thickness stretching in functionally graded plates", Composites Part B: Engineering, 56, pp. 705–716, 2014.
https://doi.org/10.1016/j.compositesb.2013.09.008

[23] Mechab, B., Mechab, I., Benaissa, S. "Analysis of thick orthotropic laminated composite plates based on higher order shear deformation theory by the new function under thermo-mechanical loading", Composited Part B: Engineering, 43(3), pp. 1453–1458, 2012.
https://doi.org/10.1016/j.compositesb.2011.11.037

[24] Radaković, A., Čukanović, D., Bogdanović, G., Blagojević, M., Stojanović, B., Dragović, D., Manić, N. "Thermal Buckling and Free Vibration Analysis of Functionally Graded Plate Resting on an Elastic Foundation According to High Order Shear Deformation Theory Based on New Shape Function", Applied Sciences, 10(12), 4190, 2020.
https://doi.org/10.3390/app10124190

[25] Akavci, S. S., Tanrikulu, A. H. "Static and free vibration analysis of functionally graded plates based on a new quasi-3D and 2D shear deformation theories", Composites Part B: Engineering, 83, pp. 203–215, 2015.
https://doi.org/10.1016/j.compositesb.2015.08.043

[26] Mechab, I., Elmeiche, N., Bernard, F. "Free Vibration Analysis of Higher-Order Shear Elasticity Nanocomposite Beams with Consideration of Nonlocal Elasticity and Poisson Effect", Journal of Nanomechanics and Micromechanics, 6(3), 04016006, 2016.
https://doi.org/10.1061/(ASCE)NM.2153-5477.0000110

[27] Eringen, A. C. "On differential equations of nonlocal elasticity andsolutions of screw dislocation and surface waves", Journal of Applied Physics, 54(9), pp. 4703–4710, 1983.
https://doi.org/10.1063/1.332803

[28] Zenkour, A. M. "Analytical solution for bending of cross-ply laminated plates under thermo-mechanical loading", Composite Structures, 65(3–4), pp. 367–379, 2004.
https://doi.org/10.1016/j.compstruct.2003.11.012

[29] Reddy, J. N. "Nonlocal theories for bending, buckling and vibration of beams", International Journal of Engineering Science, 45, pp. 288–307, 2007.
https://doi.org/10.1016/j.ijengsci.2007.04.004